DOI 10.5012/bkcs.2010.31.11.3195

Dynamics of C_{60} Molecules in Biological Membranes: Computer Simulation Studies

Rakwoo Chang* **and Jumin Lee**

*Department of Chemistry, Kwangwoon University, Seoul 139-701, Korea. *E-mail: rchang@kw.ac.kr*
Received July 16, 2010, Accepted September 7, 2010

We have performed molecular dynamics simulations of atomistic models of C_{60} molecules and DMPC bilayer membranes to study the static and dynamic effects of carbon nanoparticles on biological membranes. All four C_{60}-membrane systems were investigated representing dilute and concentrated solutions of C_{60} residing either inside or outside the membrane. The concentrated C_{60} molecules in water phase start forming an aggregated cluster. Due to its heavy mass, the cluster tends to adhere on the surface of the bilayer membrane, hindering both translational and rotational diffusion of individual C_{60}. On the other hand, once C_{60} molecules accumulate inside the membrane, they are well dispersed in the central region of the bilayer membrane. Because of the homogeneous dispersion of C_{60} inside the membrane, each leaflet is pushed away from the center, making the bilayer membrane thicker. This thickening of the membrane provides more room for both translational and rotational motions of C_{60} inside the membrane compared to that in the water region. As a result, the dynamics of C_{60} inside the membrane becomes faster with increasing its concentration.

Key Words: Fullerene, Carbon nanoparticle, DMPC membrane, Molecular dynamics simulation

Introduction

Carbon nanoparticles such as fullerenes, carbon nanotubes, and soot precursors have attracted much scientific and industrial interest regarding their characteristic structural, mechanical, and electric properties.[1-11] For example, their mechanical strength and electrical conductivity due to the delocalization of π bonds have found many applications in nano-scale electrical devices, polymer fillers, fuel cells, cosmetics, and biological sensors.

However, despite the widespread promise of these nanoparticles, especially in new technologies, research on their effect on human bodies and environment has been rare until recently.[12-19] It is therefore important to assess the potential risk issues associated with nanoparticles, such as exposure, environmental and biological fate, transport, and toxicology.[20] It is not surprising that carbon nanoparticles may be toxic in respiratory organs such as the lung, considering that it has been known for some time that their allotrope, graphite, can induce pneumoconiosis by inhalation.[21-22] Carbon nanoparticles have much larger surface area than graphite, and because of their nano-scale size, they tend to be accumulated in the interior of the body and are not eliminated by the microphage-mucociliary clearance mechanism.[15] However, systematic studies on the toxicity of carbon nanoparticles on lung tissue are absent, although a few conflicting results have been reported.[14-15,17-18,23] Adelmann *et al*.[23] reported that fullerenes are no more toxic than quartz powder from the study on the effect of fullerenes on the alveolar macrophages in vitro. Huczko *et al*.[17-18] also observed that carbon nanoparticles do not show any toxic behavior such as skin irritation, allergy, and lung toxicity. However, in the two recent experiments using mice,[14-15] single-wall carbon nanotubes were found to induce granulomas in the lung unlike graphite, which is much larger in size than carbon nanotubes.

Carbon nanoparticles can also cause serious damage to biological membranes. Sayes *et al*.[13] recently observed that pure fullerene aggregates (so-called nano-C_{60}), which are weakly soluble in water, kill human cells in culture even at very low concentrations (~ 20 ppb). This cytotoxicity tends to decrease over 7 orders of magnitude as more hydroxyl groups are attached to the fullerenes, which enhances their water solubility. It was suggested that the superoxide anions of fullerenes generated in water are responsible for membrane damage and subsequent cell death. However, cumulative experimental and theoretical studies at atomistic length scales are essential to consolidate this postulate.

Due to the recent progress in computational power, it has become routine to study realistic models of biological systems on nano-second and nano-meter scales using molecular dynamics (MD) computer simulations. These simulations provide the atomistic-level information of biological systems under study, which may be difficult to obtain from macroscopic experimental approaches. Such simulations have been successfully applied, for example, to enzyme reactions, protein folding, ion channels, and membrane fusion.[24-31]

Computer simulation studies for the interaction between carbon nanoparticles and biological materials such as proteins and DNA have also been performed.[32-38] The inhibition of the HIV-1 protease by fullerenes and their derivatives[32,36-37] was studied and the binding behavior of carbon nanotubes with nucleic acids[34,38] or amylose[33] was also investigated to improve the solubility of nanotubes. Recently, Srinivas and Klein[39] studied the interaction between a synthetic nanotube and a DMPC lipid bilayer using molecular dynamics simulations of a coarse-grained (CG) model.

However, the computational study on the effect of carbon nanoparticles on biological membranes using atomistic models has been relatively few.[40-44] Qiao *et al*.[40] performed molecular dynamics simulations to study the translocation of fullerene C_{60} and its derivative $C_{60}(OH)_{20}$ across a DPPC bilayer membrane and reported the pristine C_{60} can readily penetrate into the bilayer without a barrier in contrast to $C_{60}(OH)_{20}$. On the other hand, Smith group[41-42] studied passive transport of full-

erene C_{60} through a DMPC membrane and reported much higher free energy difference of the C_{60} permeation than that by Qiao *et al*. We have also investigated the structural and dynamical effects of both round and flat shape nanoparticles on a DMPC lipid bilayer membrane or a DPPC monolayer membrane.[43-44]

However, these previous atomistic computer simulation studies mainly focused on single-C_{60} behavior despite the fact that C_{60} readily forms an aggregate called nano-C_{60} in water phase. Notably, Wong-Ekkabut *et al*.[45] recently reported a molecular dynamics simulation study of the translocation of fullerene clusters through a model lipid membrane, although they have used a coarse-grained model for the fullerene and the lipid bilayer. Thus, in this work we have performed molecular dynamics simulations using atomic models of C_{60} clusters and DMPC bilayer membranes to have some insights into their collective effects on biological membranes.

This paper is organized as follows. In Sec. II, the molecular models and computer simulation methods used in this study are described in detail. The structural, dynamical, and thermodynamic analyses are then presented in Sec. III, followed by summary and conclusions in Sec. IV.

Methods

Molecular models. The force fields for C_{60} were generated automatically using a utility in the molecular dynamics simulation package DL-POLY,[46] which searches all possible bonding, angle, dihedral, and inversion potential sets for a given hydrocarbon configuration and assigns the corresponding DREIDING force field[47] to each potential. The DREIDING force fields are generic force fields for "nonmetallic" main-group elements (such as C, N, and O) plus H and a few metals (Na, Ca, Zn, Fe). To use a significantly long simulation time step, all bond pairs were constrained by using SHAKE.[48]

The molecular model of biological membranes used in this study is the united atom model of dimyristoylphosphatidylcholine (DMPC) lipid bilayer membranes,[49] which has been used extensively and successful in MD studies.[43,50-52] The DMPC bilayer membrane, which consists of 64 DMPC lipids, is about 34 Å thick. A total of 2000 water molecules were also included in the simulation using the TIP3P model.[53]

The initial configurations of the C_{60}-membrane systems were generated as follows. First, an artificial point atom was inserted at a position where a single C_{60} should be located inside or outside an equilibrated bilayer system. Next, the radius of the phantom atom (or the Lennard-Jones parameter σ) was gradually increased with a very small time step until the hole grows big enough to accommodate C_{60}. Then, the artificial atom was replaced by a single C_{60} and this insertion was repeated until all C_{60} molecules were inserted. The resulting configuration was equilibrated until there was no drift in simulation cell dimensions and thermodynamic quantities, such as total energy, pressure, and surface tension.

Molecular dynamics simulations.

Equilibrium MD simulations: Figure 1 shows the four C_{60}-membrane systems that are analyzed in this work. For each C_{60}-membrane geometry, two independent configurations were generated and equilibrated using the MD simulations of the

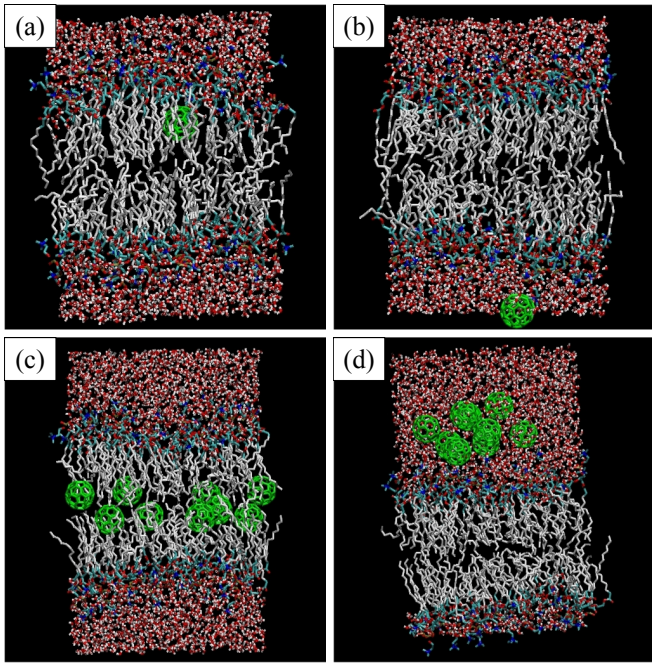

Figure 1. Representative snapshots of four systems studied in this study: a single C_{60} (a) inside or (b) outside the DMPC bilayer membrane, and nine C_{60} molecules (c) inside or (d) outside the DPMC bilayer membrane.

$NP_z\gamma T$ ensemble, where N represents the total number atoms in the simulation, P_z is the z-component of the pressure tensor, which was set to 1 bar, γ is the membrane surface tension, set to 0 N/m, and T is the system temperature, set to 308 K in this study. The MD simulations were performed in DL-POLY 2.14 modified for the $NP_z\gamma T$ ensemble. Details of the DMPC membrane model can be found elsewhere.[50]

For each C_{60}-membrane configuration, 10 ns equilibrated trajectories were saved every 1 ps and used for further analysis. The results shown in this paper are thus the averages of the two independent 10 ns trajectory runs for each case.

Umbrella sampling: To study the permeation behavior of a single C_{60} into a lipid bilayer membrane, the umbrella sampling method[54] was implemented, by which the potential of mean force (or the free energy) can be obtained along a reaction coordinate for the process of interest. More details about the method used here can be found elsewhere.[43,55]

The reaction coordinate ξ was chosen as the z-directional distance between the center of mass of a single C_{60} and the membrane center. In this method, a biased potential is additionally applied in the original molecular dynamics routine to confine the system within a small window of the reaction coordinate. In the present work, a harmonic potential, U_{umb}, with the spring constant, k_{umb}, of 10 kcal/(mol·Å^2) was used:

$$U_{umb} = \frac{1}{2} k_{umb} (\xi - z_{win})^2, \quad (1)$$

where z_{win} is the center of each window.

The initial configuration of the C_{60}-membrane system in each window was obtained by pulling it from an equilibrated configuration in the neighboring window (0.5 - 1.0 Å apart)

using U_{umb}. A total of 1 ns MD trajectories were collected in each window and the initial 50 ps of the trajectories were discarded for equilibration. The remaining 950 ps equilibrated trajectories were used to calculate the potential of mean force (pmf) profile for a narrow range of ξ within each window. 51 windows were employed at 0.5 Å intervals, spanning from ξ = 0 Å to 25 Å.

The free energy profile (or potential of mean force) for the whole range of the reaction coordinate was obtained by assembling each free energy profile in each window using the weighted histogram analysis method (WHAM).[55]

Results and Discussion

Structural properties of C_{60} clusters in DMPC membrane. Figure 1 shows representative snapshots of four C_{60}-membrane systems investigated in this study. When a single C_{60} is inserted in the membrane, it preferably resides in the hydrocarbon tail region of lipids, not the membrane center (Fig. 1(a)). This result is consistent with density profile and free energy barrier as will be discussed below, and previous studies.[40,42] This was also observed in previous simulations of flat-shape carbon nanoparticle-membrane systems, although a large round-shape carbon nanoparticle tends to be located at the membrane center.[43] The fact that C_{60} behaves similarly to a flat nanoparticle rather than a large round nanoparticle implies that the preferential location of nanoparticles is dependent more on their size (or molecular weight) than on their shape. Since the diameter of C_{60} is around 7 Å, it can reside in the hydrocarbon region without perturbing the lipid bilayer and it is also stabilized by the wrapping of neighboring hydrocarbon tails. The wrapping of nanoparticles by hydrocarbon tails is also reported in previous simulations.[44]

On the other hand, when the C_{60} concentration is high (0.1 M) as seen in Fig. 1(c), C_{60} tends to spread homogeneously near the membrane center, not at the hydrocarbon tail region, which is consistent with the previous result using a coarse-grained model.[45] This accumulation of nanoparticles in the central region of lipid bilayer membrane leads to the widening of the membrane center region, which is clearly seen in the density profiles of hydrocarbon tails of DMPC lipids as shown in Fig. 2, and as a result, affects the dynamic behavior of C_{60} significantly as will be described in detail in the following section.

A single C_{60} in water phase behaves similarly as a flat carbon nanoparticle,[43] by moving freely in both directions parallel and normal to the membrane as seen in Fig. 1(b). Whereas, C_{60} in concentrated solution tends to form an aggregated cluster, which adheres to the surface of the membrane (see Fig. 1(d)). This aggregate formation in water phase was also found in the previous coarse-grained model simulation studies.[45]

Dynamic properties of C_{60} clusters in DMPC membrane. The translational motion of C_{60} highly depends on their interesting structural behavior as discussed in the previous section. Figure 3 shows the mean square displacements of both C_{60} and a single DMPC lipid in the direction parallel to the membrane. When the nanoparticle moves inside the membrane as seen in Fig. 3(a), a single C_{60} in dilute concentration diffuses in the same pace as a single DMPC lipid. The similar behavior was also observed from the motion of a flat nanoparticle with the similar molecular weight.[43] The dynamic coupling between a single C_{60} (a flat nanoparticle) and a single DMPC lipid is the signature of the role of the particle size in the translational motion.

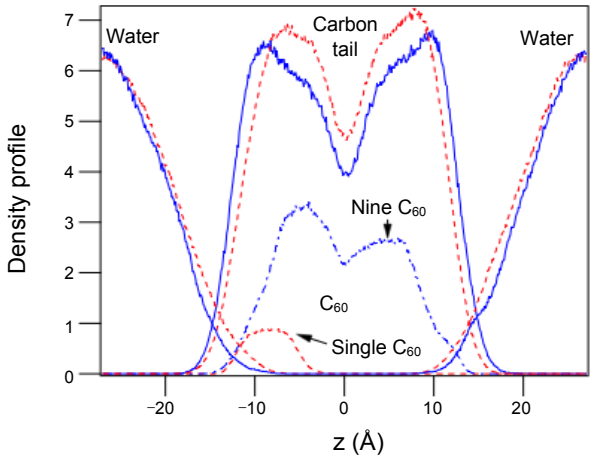

Figure 2. Number density profiles of C_{60}, the hydrocarbon tail, and water along the direction normal to the membrane when C_{60}'s are inside the membrane. Note that number density profiles of water and the hydrocarbon tail are shown for both systems: a single C_{60} (red) and nine C_{60} systems (blue).

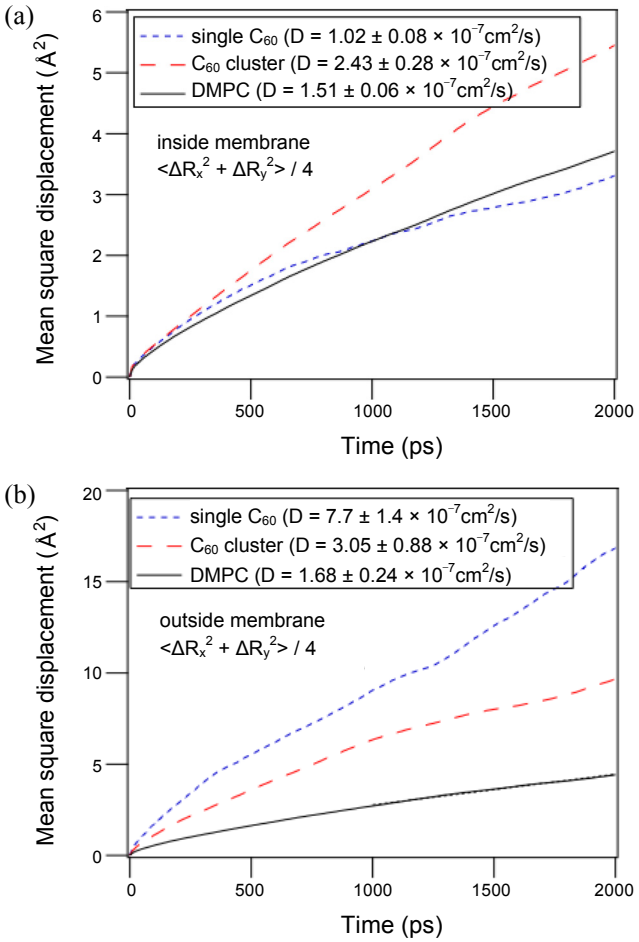

Figure 3. Mean square displacements of a single DMPC lipid and a single C_{60} molecule in the direction parallel to the membrane when C_{60}'s are (a) inside or (b) outside the membrane.

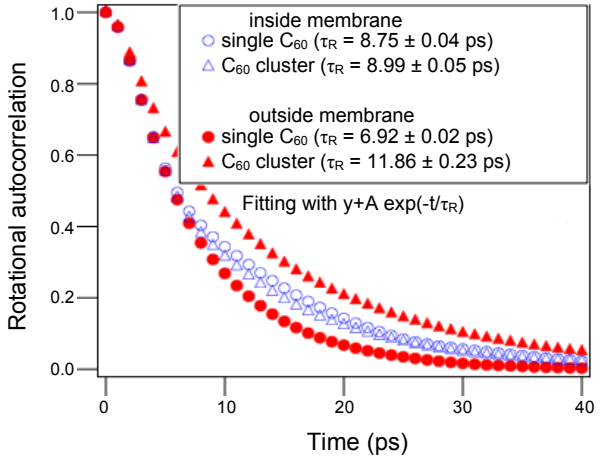

Figure 4. Rotational autocorrelation function of a single C_{60} molecule both inside and outside the membrane.

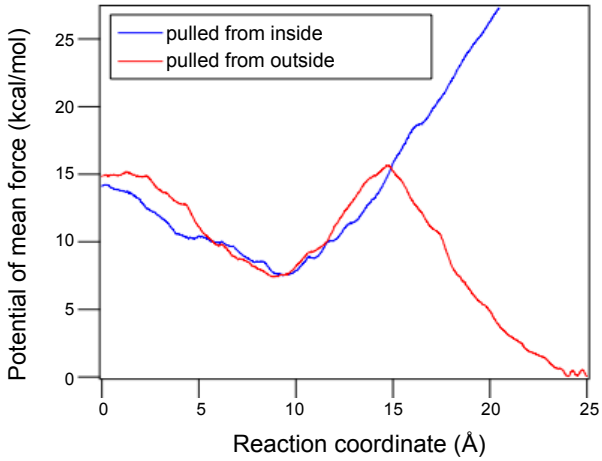

Figure 5. Potential of mean force (free energy profile) of the C_{60} permeation into the DMPC membrane.

However, in high C_{60} concentration, C_{60} moves 2.4 times as fast as that in dilute concentration. As mentioned above, this interesting phenomenon results from the widening of the membrane center region due to the presence of the dispersed fullerenes. This gap facilitates the translational motion of fullerenes in the direction parallel to the membrane plane.

On the other hand, in the water region as seen in Fig. 3(b), a single C_{60} in dilute concentration shows higher mobility than that in concentrated solution, which is the result of the cluster formation of C_{60}.

The structural behavior of C_{60} in both dilute and concentrated solutions also plays a significant role in the rotational motion of C_{60}. It has been reported that the rotational relaxation time τ of C_{60} is 3.1 ps in the gas phase and 15.5 ps in a 1,1,2,2-tetrachloroethane at 283 K.[56-57] The temperature dependence of the C_{60} rotation in the solid state can also be approximated by $\tau = \tau_0 \exp(T_a/T)$,[56] where $\tau_0 = 0.81 \pm 0.10$ ps and $T_a = 695 \pm 45$ K. According to the expression, the rotational relaxation time at $T = 308$ K is expected to be $\tau = 7.7$ ps in the solid state. We have also obtained the rotational relaxation time by fitting the time

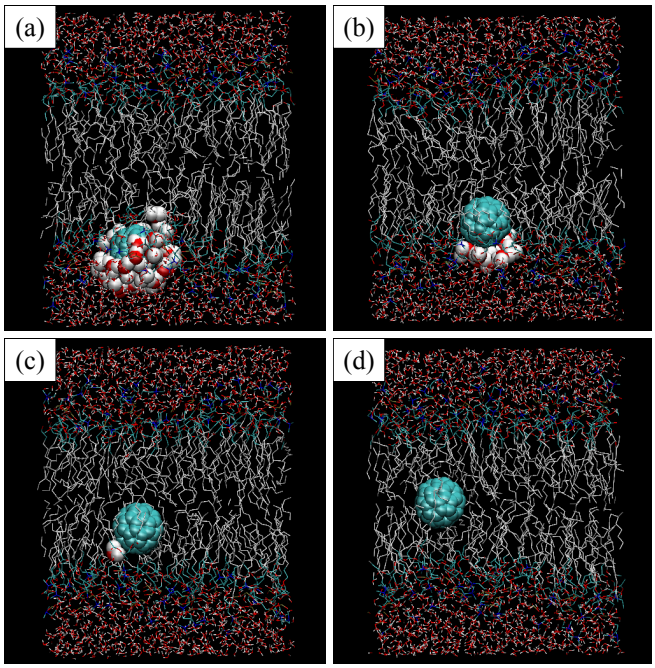

Figure 6. Representative snapshots of the C_{60}-membrane system at the reaction coordinate ξ = (a) 15 Å, (b) 10 Å, (c) 5 Å, and (d) 0 Å when the nanoparticle was initially located outside the membrane and is being pulled toward the membrane center. Note that water molecules within 5 Å of the C_{60} molecule are drawn in van der Waals spheres.

auto-correlation function of a vector, which connects two carbon atoms in the opposite position of a single C_{60} to an exponential function. The rotational auto-correlation function and the resulting relaxation times for four cases are shown in Fig. 4. Interestingly, C_{60} rotates slower inside the membrane than outside the membrane in dilute concentration. This can be understood that inside the membrane, C_{60} is wrapped by neighboring hydrocarbon tails of DMPC lipids, which hinders the rotation of C_{60}.

However, the situation becomes reversed once C_{60} starts forming a cluster: i.e., it rotates more freely inside the membrane than outside the membrane because of the widening of the bilayer membrane induced by homogeneous dispersion of C_{60}.

Permeation of C_{60} into DMPC membrane. Figure 5 shows the free energy barrier (or potential of mean force) for the C_{60} permeation into the DMPC membrane with two different pulling directions. When pulled from outside the membrane, C_{60} feels an energy barrier of around 15 kcal/mol near $\xi = 15$ Å followed by a minimum around $\xi = 10$ Å, the energy of 7.5 kcal/mol relative to the energy when it is in the water region. The presence of the free energy barrier in the permeation process is in slight disagreement with the previous simulation studies.[40,42] The origin of this discrepancy can be visualized from the snapshots of the umbrella sampling as seen in Fig. 6. When C_{60} is pulled toward the membrane from water phase, several water molecules accompany the nanoparticle even when C_{60} enters into the hydrocarbon tail region of the membrane. This adhesion of water molecules on C_{60} is not surprising because the interaction between C_{60} and water molecules is attractive.[58] However, we cannot rule out the possibility that the hydration of C_{60} in the hydrocarbon region may result from the relatively fast pulling

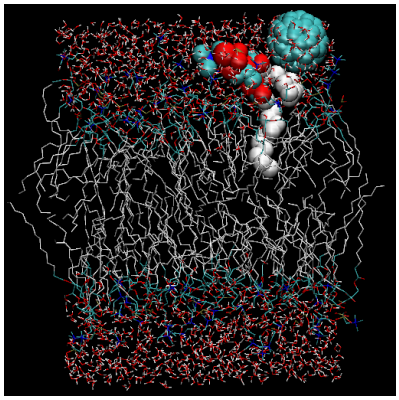

Figure 7. Representative snapshot of the C_{60}-membrane system at the reaction coordinate ξ = (a) 24.5 Å when the nanoparticle was initially located inside the membrane and is being pulled toward the water phase. Note that DMPC lipids within 5 Å of the C_{60} molecule are drawn in van der Waals spheres.

of C_{60} from the water region, which has been reported previously. [43]

When pulled further to the center of the membrane, another free energy barrier of about 7 kcal/mol shows up at $\xi = 0$ Å. The presence of local minimum at ξ = 10 Å, not at the membrane center, is also observed in the previous simulations of nanoparticle permeation.[40,42-43]

The free energy profile of the C_{60} permeation when it is pulled from the membrane center toward the water phase shows the similar behavior to that when pulled from the water region in the range of $\xi = 0$ - 15 Å: i.e., when the location of C_{60} is inside the membrane region. However, the free energy keeps increasing, as the particle is pulled further toward the water region. This discrepancy between the two free energy profiles is due to the fact that when C_{60} is pulled toward the water region, some DMPC lipid molecules, the hydrocarbon tails of which wrap around C_{60}, are pulled together as shown in Fig. 7.

Summary and Conclusions

We have performed molecular dynamics simulations of atomistic models of C_{60} clusters and a DMPC bilayer membrane to study the static and dynamic effects of carbon nanoparticles on biological membranes. In water phase, they tend to form an aggregated cluster, which makes the translational and rotational dynamics of individual C_{60} slower. On the other hand, C_{60} prefers to be dispersed rather than aggregated once it manages to get into the membrane region. This homogeneous dispersion induces the thickening of the bilayer membrane, which provides more room for both translational and rotational motions of C_{60}.

Although our molecular model does not allow any chemical reaction between nanoparticles and biological membranes, our results clearly show the permeation of carbon nanoparticles into biological membranes is feasible and once they accumulate inside the membranes, they would have significant effects on the structure of biological membranes.

Acknowledgments. This work was supported by the Korea Research Foundation Grand funded by the Korean Government (MOEHRD, Basic Research Promotion Fund) (KRF-2007-331-C00132), Korea Institute of Science and Technology Information (KSC-2009-S01-0015), and Kwangwoon Research Fund (2010).

References

1. Ajayan, P. M.; Charlier, J. C.; Rinzler, A. G. *Proc. Natl. Acad. Sci. USA* **1999**, *96*, 14199.
2. de Jonge, N.; Bonard, J. M. *Philos. Trans. R. Soc. Lond. Ser. A-Math. Phys. Eng. Sci.* **2004**, *362*, 2239.
3. Dresselhaus, M. S.; Dai, H. *MRS Bull.* **2004**, *29*, 237.
4. Lin, Y.; Taylor, S.; Li, H. P.; Fernando, K. A. S.; Qu, L. W.; Wang, W.; Gu, L. R.; Zhou, B.; Sun, Y. P. *J. Mater. Chem.* **2004**, *14*, 527.
5. Bosi, S.; Da Ros, T.; Spalluto, G.; Prato, M. *Eur. J. Med. Chem.* **2003**, *38*, 913.
6. Prato, M. Fullerene materials. In *Fullerenes And Related Structures*; Springer-Verlag: Berlin, Germany, 1999; Vol. 199, p 173.
7. Subramoney, S. *Adv. Mater.* **1998**, *10*, 1157.
8. Degiorgi, L. *Adv. Phys.* **1998**, *47*, 207.
9. Prato, M. *J. Mater. Chem.* **1997**, *7*, 1097.
10. Ball, P. *Nature* **2001**, *414*, 142.
11. Endo, M.; Hayashi, T.; Kim, Y. A.; Terrones, M.; Dresselhaus, M. S. *Philos. Trans. R. Soc. Lond. Ser. A-Math. Phys. Eng. Sci.* **2004**, *362*, 2223.
12. Colvin, V. L. *Nat. Biotechnol.* **2003**, *21*, 1166.
13. Sayes, C. M.; Fortner, J. D.; Guo, W.; Lyon, D.; Boyd, A. M.; Ausman, K. D.; Tao, Y. J.; Sitharaman, B.; Wilson, L. J.; Hughes, J. B.; West, J. L.; Colvin, V. L. *Nano Lett.* **2004**, *4*, 1881.
14. Warheit, D. B.; Laurence, B. R.; Reed, K. L.; Roach, D. H.; Reynolds, G. A. M.; Webb, T. R. *Toxicol. Sci.* **2004**, *77*, 117.
15. Lam, C. W.; James, J. T.; McCluskey, R.; Hunter, R. L. *Toxicol. Sci.* **2004**, *77*, 126.
16. Shvedova, A. A.; Castranova, V.; Kisin, E. R.; Schwegler-Berry, D.; Murray, A. R.; Gandelsman, V. Z.; Maynard, A.; Baron, P. *J. Toxicol. Env. Health Pt A* **2003**, *66*, 1909.
17. Huczko, A.; Lange, H.; Calko, E.; Grubek-Jaworska, H.; Droszcz, P. *Fullerene Sci. Technol.* **2001**, *9*, 251.
18. Huczko, A.; Lange, H.; Calko, E. *Fullerene Sci. Technol.* **1999**, *7*, 935.
19. Maynard, A. D.; Baron, P. A.; Foley, M.; Shvedova, A. A.; Kisin, E. R.; Castranova, V. *J. Toxicol. Env. Health Pt A* **2004**, *67*, 87.
20. Arnall, A. H. *Future Technologies*, *Today's Choices*; Greenpeace Environmental Trust: London, 2003.
21. Merlo, D. F.; Garattini, S.; Gelatti, U.; Simonati, C.; Covolo, L.; Ceppi, M.; Donato, F. *Occup. Environ. Med.* **2004**, 61.
22. Uragoda, C. G. *Occup. Med.-Oxf.* **1997**, *47*, 269.
23. Adelmann, P.; Baierl, T.; Drosselmeyer, E.; Politis, G.; Seidel, A.; Schwegler-Berry, D.; Steinleitner, G., *Effects of Fullerenes on Alveolar Macrophages In Vitro*; ILSI Press: Washington, DC, 1994.
24. Saiz, L.; Bandyopadhyay, S.; Klein, M. L. *Biosci. Rep.* **2002**, *22*, 151.
25. Redondo, A.; LeSar, R. *Ann. Rev. Mater. Res.* **2004**, *34*, 279.
26. Voth, G. A. *Front. Biosci.* **2003**, *8*, S1384.
27. Schlick, T.; Barth, E.; Mandziuk, M. *Annu. Rev. Biophys. Biomolec. Struct.* **1997**, *26*, 181.
28. Kohl, P.; Noble, D.; Winslow, R. L.; Hunter, P. J. *Philos. Trans. R. Soc. Lond. Ser. A-Math. Phys. Eng. Sci.* **2000**, *358*, 579.
29. Moraitakis, G.; Purkiss, A. G.; Goodfellow, J. M. *Rep. Prog. Phys.* **2003**, *66*, 383.
30. Florian, J.; Goodman, M. F.; Warshel, A. *Proc. Natl. Acad. Sci. USA* **2005**, *102*, 6819.
31. Warshel, A. *Proc. Natl. Acad. Sci. USA* **2005**, *102*, 1813.
32. Zhu, Z. W.; Schuster, D. I.; Tuckerman, M. E. *Biochemistry* **2003**,

42, 1326.
33. Xie, Y. H.; Soh, A. K. *Mater. Lett.* **2005**, *59*, 971.
34. Gao, H. J.; Kong, Y. *Annual Review Of Materials Research* **2004**, *34*, 123.
35. Noon, W. H.; Kong, Y. F.; Ma, J. P. *Proc. Natl. Acad. Sci. USA* **2002**, *99*, 6466.
36. Friedman, S. H.; DeCamp, D. L.; Sijbesma, R. P.; Srdanov, G.; Wudl, F.; Kenyon, G. L. *J. Am. Chem. Soc.* **1993**, *115*, 6506.
37. Friedman, S. H.; Ganapathi, P. S.; Rubin, Y.; Kenyon, G. L. *J. Med. Chem.* **1998**, *41*, 2424.
38. Yeh, I. C.; Hummer, G. *Proc. Natl. Acad. Sci. USA* **2004**, *101*, 12177.
39. Srinivas, G.; Klein, M. L. *Nanotechnology* **2004**, *15*, 1289.
40. Qiao, R.; Roberts, A. P.; Mount, A. S.; Klaine, S. J.; Ke, P. C. *Nano Lett.* **2007**, *7*, 614.
41. Li, L.; Davande, H.; Bedrov, D.; Smith, G. D. *J. Phys. Chem. B* **2007**, *111*, 4067.
42. Bedrov, D.; Smith, G. D.; Davande, H.; Li, L. *J. Phys. Chem. B* **2008**, *112*, 2078.
43. Chang, R.; Violi, A. *J. Phys. Chem. B* **2006**, *110*, 5073.
44. Choe, S.; Chang, R.; Jeon, J.; Violi, A. *Biophys. J.* **2008**, *95*, 4102.
45. Wong-Ekkabut, J.; Baoukina, S.; Triampo, W.; Tang, I.-M.; Tieleman, D. P.; Monticelli, L. *Nature Nanotech.* **2008**, *3*, 363.
46. Smith, W.; Forester, T. R. *J. Molec. Graphics* **1996**, *14*, 136.
47. Mayo, S. L.; Olafson, B. D.; Goddard, W. A., III. *J. Phys. Chem.* **1990**, *94*, 8897.
48. Ryckaert, J. P.; Ciccotti, G.; Berendsen, H. J. C. *J. Comput. Phys.* **1977**, *23*, 327.
49. Smondyrev, A. M.; Berkowitz, M. L. *J. Comput. Chem.* **1999**, *20*, 531.
50. Chang, R. W.; Ayton, G. S.; Voth, G. A. *J. Chem. Phys.* **2005**, *122*, 244716.
51. Smondyrev, A. M.; Berkowitz, M. L. *J. Chem. Phys.* **1999,** *110*, 3981.
52. Smondyrev, A. M.; Voth, G. A. *Biophys. J.* **2002**, *82*, 1460.
53. Jorgensen, W. L.; Chandrasekhar, J.; Madura, J. D.; Impey, R. W.; Klein, M. L. *J. Chem. Phys.* **1983**, *79*, 926.
54. Torrie, G. M.; Valleau, J. P. *J. Comput. Phys.* **1977**, *23*, 187.
55. Roux, B. *Comput. Phys. Commun.* **1995**, *91*, 275.
56. Johnson, R. D.; Yannoni, C. S.; Dorn, H. C.; Salem, J. R.; Bethune, D. S. *Science* **1992**, *255*, 1235.
57. Johnson, R. D.; Bethune, D. S.; Yannoni, C. S. *Acc. Chem. Res.* **1992**, *25*, 169.
58. Li, L.; Bedrov, D.; Smith, G. D. *J. Phys. Chem. B* **2006**, *110*, 10509.